Aalborg Universitet

Opsonophagocytosis of Chlamydia pneumoniae by human monocytes and neutrophils

Lausen, Mads; Pedersen, Mathilde Selmar; Rahman, Nareen Sherzad Kader; Holm-Nielsen, Liv Therese; Farah, Faduma Yahya Mohamed; Christiansen, Gunna; Birkelund, Svend

Published in:
Infection and Immunity

DOI (link to publication from Publisher):
10.1128/IAI.00087-20

Publication date:
2020

Document Version
Accepted author manuscript, peer reviewed version

IAI Accepted Manuscript Posted Online 13 April 2020
Infect. Immun. doi:10.1128/IAI.00087-20

Opsonophagocytosis of *Chlamydia pneumoniae* by human monocytes and neutrophils

Mads Lausen[a], Mathilde Selmar Pedersen[a], Nareen Sherzad Kader Rahman[a], Liv Therese Holm-Nielsen[a], Faduma Yahya Mohamed Farah[a], Gunna Christiansen[a,b], Svend Birkelund[a#]

[a]Department of Health Science and Technology, Aalborg University, Fredrik Bajers Vej 3b, 9220 Aalborg Ø, Denmark

[b]Department of Biomedicine, Aarhus University, Wilhelms Meyers Allé 4, 8000 Aarhus, Denmark

[#]Corresponding author: sbirkelund@hst.aau.dk

Word count abstract: 249

Word count main text: 4686

Running title: Opsonization and phagocytosis of *C. pneumoniae*

Keywords: Chlamydia pneumoniae, opsonization, phagocytosis, monocytes, neutrophils

ABSTRACT

The human respiratory tract pathogen *Chlamydia pneumoniae* (*C. pneumoniae*) causing mild to severe infections have been associated with the development of chronic inflammatory diseases. To understand the biology of *C. pneumoniae* infections several studies have investigated the interaction between *C. pneumoniae* and professional phagocytes. However, these studies have been conducted under non-opsonizing conditions making the role of opsonization in *C. pneumoniae* infections elusive. Thus, we analyzed complement and antibody opsonization of *C. pneumoniae* and evaluated how opsonization affects chlamydial infectivity and phagocytosis in human monocytes and neutrophils.

We demonstrated that IgG antibodies and activation products of complement C3 and C4 are deposited on the surface of *C. pneumoniae* elementary bodies when incubated in human serum. Complement activation limits *C. pneumoniae* infectivity *in vitro* and have the potential to induce bacterial lysis by formation of the membrane attack complex. Co-culture of *C. pneumoniae* and freshly isolated human leukocytes showed that complement opsonization is superior to IgG opsonization for efficient opsonophagocytosis of *C. pneumoniae* in monocytes and neutrophils. Neutrophil-mediated phagocytosis of *C. pneumoniae* was crucially dependent on opsonization while monocytes retain minor phagocytic potential under non-opsonizing conditions. Complement opsonization significantly enhanced the intracellular neutralization of *C. pneumoniae* in peripheral blood mononuclear cells and neutrophils and almost abrogated the infectious potential of *C. pneumoniae*. ‘

In conclusion, we demonstrated that complement limits *C. pneumoniae* infection *in vitro* by interfering with *C. pneumoniae* entry into permissive cells, by direct complement-induced lysis and by tagging bacteria for efficient phagocytosis in both monocytes and neutrophils.

INTRODUCTION

Chlamydia pneumoniae (*C. pneumoniae*) is a human pathogen frequently causing mild respiratory symptoms during infection that usually resolves spontaneously but can cause severe, long-lasting atypical pneumonia and has been associated with the development of several chronic disease conditions including atherosclerosis and asthma (1, 2). *C. pneumoniae* is an obligate intracellular Gram-negative bacterium with a unique biphasic developmental cycle. The bacterium alternates between the extracellular infectious elementary body (EB) and the intracellular non-infectious reticular body (RB). During infection, *C. pneumoniae* EBs engage airway epithelium and induce their own uptake by secreting pre-formed effectors into the host cell cytoplasm by the type-III secretion system (3). Intracellularly, the EBs transform into RBs and start replicating in a modified vacuole called an inclusion. After 48-72 hours RBs start to divide asynchronously and EBs are formed and released from the host cell by cell lysis or by membrane extrusion (4).

Upon infection, *C. pneumoniae* EBs first encounter airway epithelial cells and alveolar macrophages which respond to infection by secreting inflammatory mediators stimulating vascular endothelium activation and immune cell chemotaxis (5). Neutrophil granulocytes are the first immune cells to transmigrate from the blood stream into the alveolar space and subsequently signal for mononuclear cell recruitment and infiltration (6, 7). Thus, neutrophils and monocytes comprise an early cellular defense against *C. pneumoniae* and the interaction between extracellular chlamydial EBs and these phagocytes likely determines the course of the infection. Multiple studies have proposed that *C. pneumoniae* can evade intracellular killing mechanisms in both monocytes and neutrophils and thereby use these cells as cellular vectors for extrapulmonary dissemination potentially causing chronic disease (8–10). However, these pro-survival mechanisms may be altered by the route of bacterial ingestion since engagement with different phagocytic receptors activates different intracellular signaling and trafficking pathways.

It was previously shown that phagocytic uptake of the intracellular bacterium *Mycobacterium tuberculosis* (*M. tuberculosis*) through complement receptors or the mannose receptor protects the bacterium from intracellular killing by delaying phagosome maturation (11, 12). On the contrary, uptake of antibody opsonized *M. tuberculosis* trough Fcγ-receptors causes rapid phagosome maturation and phagolysosomal fusion leading to reduced infection outcome. Thus, opsonin-directed phagocytosis is a critical factor determining the intracellular fate of *M. tuberculosis* and similar mechanisms could be involved in *C. pneumoniae* infections and pathogenesis, despite these pathogens being very different in nature.

The complement system consists of more than 30 soluble and membrane-bound proteins that works in a cascade-like manner to induce anti-microbial effector functions including opsonization, chemotaxis and cell lysis. The cascade process is initiated within minutes of engagement (13) and proceeds through three separate activation pathways: Classical- (recognition of antibody complexes), lectin- (recognition of carbohydrate moieties), and alternative pathway (spontaneous hydrolysis of C3) (14). Following activation, complement C4 and C3 are proteolytically cleaved into small soluble C4a/C3a fragments (9 kDa each) and large C4b/C3b fragments (75 kDa and 110 kDa, respectively) that attach covalently to the activating surface and opsonize the microbe for phagocyte detection. C3b can be further cleaved into iC3b, C3dg or C3d, which are all potent opsonins recognized by different complement receptors on phagocytic cells (14). The final stage of the complement cascade includes cleavage of complement C5 and generation of a multimeric membrane-spanning C5b-9 complex (membrane attack complex, MAC) that induces pore formation and cell lysis (14).

During primary infection, *C. pneumoniae* engages the complement system in the alveolar space. Although alveolar complement concentration and activity is reduced compared to concentrations and activity seen in serum, the system is sufficiently functional to opsonize *M. tuberculosis* with complement C3 activation products (15, 16). Primary infection leads to *C. pneumoniae*-specific IgG production, but these antibodies offers limited protection against *C. pneumoniae* since reinfections are frequently observed (17). Thus, during secondary infections both antibodies and complement are present in the alveolar space, which have the potential to modulate the intracellular fate of *C. pneumoniae* in phagocytes and hence the outcome of the infection.

To further characterize the pathogenesis of *C. pneumoniae* during primary and secondary infections we investigated how complement- and antibody opsonization affect phagocytosis and intracellular survival of *C. pneumoniae* in human monocytes and neutrophils.

RESULTS

Complement- and antibody opsonization of *C. pneumoniae*

To examine the role of opsonization and phagocytosis during *C. pneumoniae* infections, we first screened the serum from 10 healthy donors for IgG antibodies against *C. pneumoniae* and found that nine out of ten donors were positive for IgG against *C. pneumoniae*. Serum from one seropositive individual and serum from the only identified seronegative individual were used in all further experiments. These sera are called immune serum and non-immune serum, respectively, throughout this paper.

Different cleavage fragments of complement C3 and C4 are known to bind and opsonize bacteria for phagocytic recognition. C3 deposition on *C. pneumoniae* has only been investigated by flow cytometry using an antibody recognizing various C3 cleavage forms (18). Thus, the exact C3 opsonins that bind the *C. pneumoniae* surface remain unknown. In addition, complement C4 deposition has never been investigated on *C. pneumoniae*. We therefore analyzed the deposition of these complement components on purified *C. pneumoniae* EBs using immunoelectron microscopy (IEM) and western blotting.

Figure 1A demonstrates that complement C3 is abundantly deposited on the chlamydial surface when incubated in non-immune serum (NHS-). Very limited C3 deposition was observed in heat-inactivated serum (HIHS-) (Fig. 1B) suggesting that C3 deposition was due to activation of the complement system and not due to unspecific antibody binding This observation was confirmed by quantification of gold particles showing a median gold-binding ratio of 21.8 in NHS- (12.1-20.9) vs. 1.9 in HIHS- (1.2-2.6) (Fig. 1C).

These observations were confirmed by western blot analysis demonstrating solid deposition of C3 in NHS-, but not in HIHS- (Fig. 1D). Several high molecular bands (above 110 kDa) are seen on the western blot, indicating cleavage of the alpha chain of native C3 and covalent attachment of C3 fragments to chlamydial surface structures (Fig. 1D). The 40 kDa fragment shown in Fig. 1D corresponds to the α'2 chain of C3, demonstrating deposition of the potent opsonin iC3b. Interestingly, we also demonstrated deposition of C4 on the chlamydial surface when incubated in NHS- (Fig. 1E), but not in HIHS- (Fig. 1F). Compared to C3, C4 was more sporadically deposited on the chlamydial surface indicated by a lower bacteria-to-background ratio for C4 (Fig. 1E+G). The observations were confirmed by western blot analysis which demonstrated deposition of the C4b opsonin. C4b deposition is indicated by the emergence of high molecular bands suggesting cleavage and exposure of the thioester group in the alpha chain of C4 along with the presence of the C4 beta- (70 kDa) and gamma chains (35 kDa) (Fig. 1H). These observations suggest involvement of the lectin-mediated pathway since the non-immune serum tested negative for both anti-*C. pneumoniae* IgG and IgM making classical-mediated C4 activation unlikely.

To evaluate opsonization during secondary infection we incubated *C. pneumoniae* EBs in immune-serum and investigated both antibody- and complement opsonization. Immunofluorescence microscopy demonstrated that immune serum reacted with individual chlamydial organisms located in perinuclear inclusions in infected HeLa cells (Fig. 2A). The IgG antibodies reacted with the surface of RBs indicated by the ring-shaped structures surrounding a DNA core (Fig, 2A). As expected, non-immune serum did not react with the chlamydial inclusions (Fig. 2B). These observations were made on fixed and permeabilized cells and may not accurately reflect native surface labeling.

Thus, to investigate native antibody labeling and to determine if antibodies in immune-serum also bind *C. pneumoniae* EBs, we incubated purified *C. pneumoniae* EBs with immune-serum and evaluated IgG binding to the surface by IEM. Gold-conjugated anti-human IgG antibodies bind to the surface of chlamydial EBs when incubated in immune-serum (Fig. 2C), while only few gold particles were associated with chlamydial EBs when incubated in non-immune serum (Fig. 2D). Quantitative analysis demonstrated a median gold-binding ratio of 27.1 (23.6-39.1) in HIHS+ vs. 1.1 (0.6-2.5) in HIHS-, showing that the limited bacterial gold deposition observed in non-immune serum equals the background gold deposition (Fig. 2E). Thus, human *C. pneumoniae* IgG antibodies present in serum interact with epitopes located both on fixed RBs (Fig. 2A) and native EBs (Fig. 2C+E).

Next, we wanted to investigate if anti-*C. pneumoniae* IgG affects complement activation and deposition on the chlamydial surface. Complement C3 was heavily deposited when *C. pneumoniae* were incubated in NHS+, but not in HIHS+ (Fig. 2F-H). Similar levels of C3 deposition between immune serum and non-immune serum were observed (median ratios: NHS-: 21.8 vs. NHS+: 23.8) suggesting a negligible role of IgG in complement C3 deposition (Fig. 1A+C and Fig 2F+H).

As expected, complement C4 was deposited on *C. pneumoniae* incubated in NHS+, but not in HIHS+ (Fig. 2J-L). More complement C4 deposition was observed in immune serum, in the presence of IgG, compared to non-immune serum (median ratios: NHS-: 3.5 vs. NHS+: 27.5) suggesting increased classical complement activation.

Increased complement C4 deposition in immune serum compared to non-immune serum was also indicated by western blot analysis demonstrating more intense C4 bands when bacteria were incubated in immune-serum (Fig. 2M vs. Fig. 1H). Several high molecular bands were observed suggesting cleavage of the alpha chain of C4 and covalent attachment of C4b to the bacterial surface. In addition, the cleaved alpha chain (a' chain) was observed around 80 kDa suggesting non-covalent attachment of C4b (Fig. 2M).

In summary, *C. pneumoniae* is opsonized by iC3b and C4b in the absence of anti-*C. pneumoniae* IgG. *C. pneumoniae* IgG is able to bind both EBs and RBs leading to increased C4b deposition on purified EBs.

Complement-mediated bacterial lysis

We wanted to investigate if the initial binding of complement and antibodies alone could interfere with reproductive infection of *C. pneumoniae*, since antibody binding and complement activation precede immune cell infiltration.

Electron microscopy revealed that most chlamydial organisms were intact after 30 minutes of incubation in serum, demonstrating no signs of bacterial lysis (Fig. 3A). However, few bacteria showed signs of complement-mediated lysis indicated by disruption of normal bacterial morphology together with pore-forming structures (Fig. 3B, arrowheads). Thus, we aimed to investigate if the complement cascade proceeds through the terminal complement pathway leading to MAC-induced bacterial lysis in these cases. Chlamydial organisms were incubated in non-immune- and immune serum and immunogold-labeled using a monoclonal antibody, recognizing a neoepitope of the C5b-9 complex. As shown in Fig. 3C, C5b-9 is asymmetrically deposited on disintegrated chlamydial organisms and is located in close proximity to 10 nm pore-like structures indicating MAC formation and MAC-induced lysis. Bacteria incubated in heat-inactivated serum showed no signs of bacterial lysis (Fig. 3D). MAC formation was observed in both immune- and non-immune serum, but more gold was observed in

NHS+ samples (median ratio: 34.5 (12.0-72.4)) compared to NHS- samples (median ratio: 12.1 (6.0-36.2)), suggesting that serum IgG promotes formation of C5b-9 complexes. Interestingly, most gold-labeled bacteria appeared healthy, with normal morphological features, and with no signs of bacterial lysis. These observations suggest that non-lytic C5b-9 complexes are formed on the chlamydial surface. Chlamydial organisms with altered morphology and signs of bacterial lysis appeared generally larger than unaffected chlamydiae possibly representing intermediate- or reticular bodies inevitably located within the EB fraction during the EB purification process. These observations imply that lytic C5b-9 formation occurs primarily on intermediate- or reticular bodies but leaving EBs unaffected. Thus, some *C. pneumoniae* organisms are sensitive to complement-mediated lysis in both immune and non-immune serum.

Our observations show that complement fragments and antibodies deposit on almost all *C. pneumoniae* EBs while only few bacteria are directly killed by complement-mediated lysis. We therefore asked if opsonin deposition on apparently intact *Chlamydia* EB had any effect on chlamydial infectivity. To answer this question, we tested the ability of immune- and non-immune serum to neutralize chlamydial infection in HeLa cells by enumerating inclusion forming units (IFU) in each experimental condition. Figure 4 shows that complement had a significant impact on chlamydial infectivity. Only 0.38% ± 0.2 (mean ± SD) and 1.19% ± 0.72 of the initial inoculum was recovered after incubation in immune- (NHS+) and non-immune serum (NHS-), respectively. These observations indicate that the combination of complement and antibodies more efficiently reduces chlamydial infectivity than complement alone, but the difference was not statistically significant. When serum was heat-inactivated 19.1% ± 6.7 and 44.7% ± 5.8 (Fig. 4) of inoculum was recovered demonstrating that complement significantly inhibits *C. pneumoniae* infectivity. The difference between heat-inactivated immune-

(HIHS+) and non-immune serum (HIHS-) further suggests that antibodies alone can reduce *C. pneumoniae* infectivity. To confirm this observation, we supplemented heat-inactivated non-immune serum (HIHS-) with the IgG fraction from a seropositive donor and evaluated chlamydial infectivity. As shown in Figure 4, supplementing non-immune serum with anti-*C. pneumoniae* IgG (HIHS-+IgG) significantly reduced chlamydial infectivity compared to non-immune serum alone confirming that anti-*C. pneumoniae* IgG reduces infectivity of *C. pneumoniae*. These data demonstrate that both antibody-, but especially complement opsonization have profound impact on *C. pneumoniae* infectivity.

Complement-mediated phagocytosis of *C. pneumoniae*

As demonstrated above, neither complement- nor antibody opsonization completely abrogates chlamydial infectivity. We therefore aimed to investigate how phagocytes participate in the clearance of opsonized *C. pneumoniae*. To quantitatively evaluate the role of opsonization in phagocytic uptake during primary and secondary infections, we analyzed the uptake of opsonized and non-opsonized *C. pneumoniae* EB in monocytes and neutrophils by flow cytometry. Intracellular staining of cells for flow cytometry is troublesome as it requires cell permeabilization which causes considerable changes to physical characteristics of the cells. To avoid permeabilization *C. pneumoniae* organisms were labeled by FITC and uptake of FITC-labeled bacteria and FITC-labeling specificity were evaluated by confocal microscopy.

Figure S1 shows that FITC-labeled organisms appear small (around 0.5 µm) and round in accordance with the morphology of chlamydial EBs. To confirm the intracellular location of these FITC-signals, monocytes were stained for the cytoplasmic protein S100A8 to visualize the cell cytoplasm (Fig. S1B). As demonstrated in Fig. S1C all FITC-positive organisms are located inside the cell cytoplasm.

FITC-labeling is a rather unspecific fluorescent labeling technique since the isothiocyanate group reacts with primary amine groups. Thus, to evaluate whether the FITC-signal in Fig. S1 originates from chlamydial organisms and not contaminants like cell debris from the chlamydial isolation procedure, we stained FITC-labeled chlamydiae with a monoclonal antibody against chlamydial LPS. As demonstrated in Fig. S1D+F all FITC-positive structures reacted with the anti-*Chlamydia* LPS antibody confirming that all FITC-positive structures are chlamydial organisms. Thus, FITC-labeling of *C. pneumoniae* is efficient and specific and the FITC-labeled bacteria locate inside the cells enabling the bacteria to be used in a flow cytometric assay.

To analyze the effect of opsonization on phagocytosis of *C. pneumoniae*, isolated leukocytes were incubated with FITC-labeled *C. pneumoniae* in 30 min under different opsonizing conditions and subjected to flow cytometry analysis. To quantify the uptake, monocyte and neutrophil cell populations were gated as demonstrated in Fig. S2. Both cell types were gated based on forward- and side-scatter characteristics and monocytes were additionally gated based on CD14 surface expression.

We first analyzed the role of complement-mediated opsonophagocytosis to experimentally mimic the infection conditions during primary infection. Thus, phagocytic uptake was quantified in medium containing either normal non-immune serum (NHS-) or heat-inactivated non-immune serum (HIHS-). As depicted in Fig. 5A+B, phagocytosis of *C. pneumoniae* in both monocytes and neutrophils is much more efficient in NHS- compared to HIHS- suggesting an important role for complement opsonization in phagocytosis of *C. pneumoniae*. Interestingly, neutrophil-mediated phagocytosis was almost absent under non-opsonizing conditions (Fig 5B, HIHS-), suggesting that opsononization is paramount for neutrophil phagocytosis of *C. pneumoniae* while monocytes exploit opsonin-independent phagocytic pathways.

Phagocytosis in the presence of anti-chlamydial antibodies

We demonstrated that monocyte- and especially neutrophil-mediated phagocytosis of *C. pneumoniae* were critically dependent on complement opsonization. Complement activation and activity in the alveolar space is reduced compared to serum and is primarily dependent on classical complement activation (15, 16). Thus, we sought to investigate whether anti-*C. pneumoniae* antibodies could mediate efficient phagocytosis or potentiate complement-mediated phagocytosis as both mechanisms may be important to understand the biology of *C. pneumoniae* reinfections.

By comparing the heat-inactivated immune serum (Fig 5C+D, HIHS+) with heat-inactivated non-immune serum (Fig 5A+B, HIHS-) it is evident that antibody opsonization increased phagocytic uptake of *C. pneumoniae* in both monocytes (3-fold increase) and especially in neutrophils (17-fold increase), however this effect was significantly lower compared to complement alone. To confirm these observations, we purified the IgG-fraction from immune serum and supplemented HIHS- with purified IgG. As demonstrated in Fig. 5E+F, supplementing non-immune serum with the IgG-fraction from immune serum increased the phagocytic uptake in both monocytes and neutrophils, confirming that the observed differences are due to anti-*C. pneumoniae* antibodies. We could not assess whether the presence of IgG potentiated complement-mediated phagocytosis since both monocyte and neutrophil cell populations were saturated with bacteria when complement competent serum was used (Fig. 5A-D, NHS+/-). We therefore re-analyzed these samples using *C. pneumoniae* at MOI=1 and showed that monocytes and neutrophils more efficiently ingest *C. pneumoniae* when both complement and IgG antibodies are present (Fig. 5G+H).

Intracellular survival of ingested bacteria

C. pneumoniae is ingested through both complement- and antibody dependent mechanisms. Evidence from other intracellular bacteria shows that the intracellular fate of ingested bacteria is highly dependent on the route of uptake, and it is therefore important to study the intracellular fate of *C. pneumoniae* under the opsonizing conditions we have demonstrated here.

To evaluate the intracellular fate of ingested bacteria, PBMCs and neutrophils containing opsonized and non-opsonized bacteria were lysed by ultrasonication and liberated bacteria were used to infect HeLa cell monolayers.

Statistically significantly less IFU were recovered when bacteria were ingested by PBMCs in the presence of immune serum (NHS+: 45 ±19 IFU/µl) and non-immune serum (NHS-: 70 ±16 IFU/µl) compared to bacteria ingested in media supplemented with heat-inactivated immune serum (HIHS+: 315 ±49 IFU/µl) and non-immune serum (HIHS-: 452 ±25 IFU/µl) (Fig. 6A). Similar results were obtained for neutrophils with 99 ±4 IFU/µl and 141 ± 32 IFU/µl recovered IFU in immune- and non-immune serum, respectively (Fig. 6B). Serum heat-inactivation caused a statistically significant increase in IFU recovery from both immune serum (Fig. 6B, HIHS+: 452 ±139 IFU/µl) and non-immune serum (Fig. 6B, HIHS-: 1151 ±259 IFU/µl). Although more bacteria are present intracellularly in cells incubated in NHS compared to HIHS (Figure 5A-D) more reproductive bacterial organisms can be recovered from cells in HIHS. These data suggest that complement not only facilitate rapid and efficient uptake of *C. pneumoniae*, but also mediates effective intracellular neutralization. We also observed statistically significant less IFU recovered from bacteria ingested in the presence of heat-inactivated immune serum (HIHS+) compared to heat-inactivated non-immune (HIHS-) in both cell types (Fig. 6A+B) suggesting that antibodies also play a role in bactericidal activity against *C. pneumoniae*.

Studies performed on *M. tuberculosis* suggest that bacterial uptake by complement receptors delays phagosomal maturation and phagolysomal fusion thereby facilitating intracellular bacterial survival. Our results suggest the opposite; that complement-mediated uptake leads to rapid intracellular neutralization of *C. pneumoniae*. We therefore tested whether *C. pneumoniae* were targeted to lysosomal compartments in monocytes after complement-mediated ingestion. Figure 6C-E shows that *C. pneumoniae* localizes within LAMP1-positive vesicular structures in monocytes after 30 min incubation in media supplemented with non-immune serum (NHS-). Staining of mock infected cells demonstrates that FITC-signal in LAMP1-positive structures originates from chlamydial organisms (Fig. 6F). Thus, complement-mediated uptake of *C. pneumoniae* in monocytes directs ingested bacteria to lysosomal compartments.

DISCUSSION

In the present study, we demonstrated that *C. pneumoniae* EBs are opsonized with both IgG and the complement opsonins iC3b and C4b when incubated in human serum. We showed that complement activation limits *C. pneumoniae* infection in multiple ways by interfering with *C. pneumoniae* entry into permissive cells, by direct MAC-induced lysis and by tagging bacteria for efficient phagocytosis by both monocytes and neutrophils.

The activation and deposition of complement C3 and the terminal complement complex on *C. pneumoniae* demonstrated in this study were previously shown by Cortes and colleagues (18). Interestingly, using electron microscopy, we observed C5b-9 deposition without pore-formation and bacterial lysis. C5b-9 complexes associated with pore-like structures and altered bacterial morphology were primarily observed on reticular- and intermediate bodies. Thus, our observations suggest that extracellular EBs may be resistant to MAC-induced lysis. It is likely, that the cysteine-rich proteins in the highly cross-linked chlamydia outer membrane of EBs provide a physical barrier that hinders components of the terminal complement complex to interact with the outer membrane lipid bilayer. Alternatively, MAC formation could be inhibited by recruitment of host-derived complement regulators to the EB surface. Thus, it was previously demonstrated that *C. trachomatis* binds the MAC-inhibitor vitronectin, however, it was not investigated if vitronectin modulates complement deposition on the chlamydial surface (19).

Cortes et al. concluded that properdin and alternative complement activation was indispensable for C3b deposition and complement-mediated neutralization. Interestingly, we found that complement C4 is deposited on the surface of *C. pneumoniae*. Deposition of complement C4 in both immune- and nonimmune serum suggests that also the lectin-mediated activation pathway is involved in *C.*

pneumoniae induced complement activation. This observation is supported by previous studies demonstrating that different lectins can bind the surface of *C. pneumoniae* (20, 21). Moreover, quantification of gold-labeling and semi-quantitative western blot analysis suggested that more C4 was deposited in immune serum compared to non-immune serum, indicating activation of the classical pathway. This is supported by the finding that IgG1 is the predominant IgG subclass raised against *C. pneumoniae* and to a lesser extend IgG3 and both IgG1 and IgG3 are efficient complement activators (22). The IgG subclasses raised against *C. pneumoniae* may also explain why we observe an IgG-dependent inhibition of *C. pneumoniae* infectivity in HeLa cells (Fig. 4). Studies on *C. trachomatis* showed that HeLa cells express FcγRIII and that Fc-mediated endocytosis through this receptor promotes reproductive infection of *C. trachomatis* (23, 24). It is likely that *C. trachomatis* is more prone to FcγRIII-mediated uptake compared to *C. pneumoniae* since IgG3 is the predominant IgG subclass raised against *C. trachomatis* (22). Thus, the IgG subclass distribution seems important for the infectivity and reproductive outcome of *Chlamydia spp. in vitro.*

A possible explanation for the discrepancies between our results and the findings by Cortes et al. could be that classical- and/or lectin-mediated activation pathways are abrogated at the C4 level leading to pathway termination before C3 cleavage. C4 binding protein (C4bp), a fluid-phase negative complement regulator, can terminate complement activation at the C4 level by inducing C4b cleavage and C2a dissociation from the classical C3 convertase (25). Several bacterial pathogens are able to recruit and bind C4bp leading to complement resistance, but this has not yet been demonstrated for chlamydial organisms (26, 27).

The alternative activation pathway seems important for *C. pneumoniae*-induced complement activation *in vitro* but the significance of this pathway during *in vivo* lung infections is still elusive. In the lungs, complement activation proceeds primarily through the classical pathway and alternative complement activation fails to activate and deposit C3 on both mycobacteria and streptococci in bronchoalveolar lavage fluid (15, 28). It remains uncertain whether *C. pneumoniae* is opsonized in the alveolar space of the lungs, but the classical complement activation is functional, and during secondary infection complement activating IgG is present in the alveolar space (15).

We show that complement efficiently facilitates phagocytosis of *C. pneumoniae* in both monocytes and neutrophils and that most opsonized bacteria are unable to cause reproductive infection when liberated from phagocytes. Complement receptor 3 (CR3, CD11b/CD18) recognizes different C3 cleavage fragments including iC3b identified on *C. pneumoniae* EBs here. CR3 is, together with Fcγ-receptors, the most important phagocytic receptor and is widely expressed on both monocytes and neutrophils. It is, therefore, likely that complement-mediated phagocytosis takes place via CR3 leading to intracellular destruction. This is different from CR-mediated uptake of other intracellular bacteria. CR-mediated uptake of *M. tuberculosis* into human monocytes and macrophages allow safe entrance by delaying phagosomal maturation and phagolysosomal fusion (11). We observed that *C. pneumoniae* is rapidly targeted to LAMP1-positive intracellular compartments showing efficient phagosomal trafficking facilitating intracellular neutralization of the chlamydial reproductive potential. Thus, safe entrance into host cells through CR-mediated phagocytosis is not a conserved mechanism for all intracellular bacteria. This is supported by the observation that the facultative intracellular bacterium *Francisella tularensis* (*F. tularensis*) fails to escape phagosomal trafficking in murine bone-marrow macrophages when opsonized with either complement or IgG (29). Knockout of CD11b, a subunit of the heterodimeric CR3, leads to phagosomal escape with cytosolic localization of *F. tularensis*, supporting that CR3 plays opposing roles during experimental infections with different intracellular bacteria (29).

Direct interaction between opsonized bacteria and phagocytic opsonin-receptors provides one explanation for the increased phagocytic uptake and intracellular neutralization observed here. Phagocytic priming by the complement anaphylatoxins C3a and C5a may provide another likely explanation. In an *in vivo C. psittaci* lung infection model C5aR$^{-/-}$ mice displayed slightly worsened clinical score compared to WT during early stage infection (30). The same authors later demonstrated that C3a and its receptor C3aR are critically involved in anti-chlamydial immunity in the same *C. psittaci* lung infection model (31). Both receptors are expressed on monocytes and neutrophils and can potentiate phagocytic functions by inducing both an increased surface expression of complement receptors and induce a hostile intracellular environment (32, 33). C5a induces increased surface expression of CD11b and increased phagocytosis of *Escherichia coli* (*E. coli*) in neutrophils (34) and can also potentiate intracellular killing of *E. coli* by increasing the oxidative burst in a whole blood assay (35).

In addition, priming neutrophils with C5a leads to translocation of CR1 containing secretory vesicles to the cell surface (36, 37). CR1 recognizes the activation products C3b and C4b together with several other complement-related proteins (38). We demonstrate for the first time, that C4b is deposited on the surface of *C. pneumoniae* and hence, C5a-induced translocation of CR1 to the plasma membrane may induce increased bacterial phagocytosis. However, the role of C4b in opsonophagocytosis remains elusive.

We demonstrated that *C. pneumoniae* ingested in the presence of complement-competent serum had impaired ability to cause reproductive infection in HeLa cells compared to bacteria ingested under non-opsonizing conditions. Intracellular survival and replication of *C. pneumoniae* within phagocytes have previously been evaluated in several *in vitro* studies; however, these have been conducted under various experimental conditions. Both *C. pneumoniae* and *C. trachomatis* are able to replicate in human neutrophils when ingested under non-opsonizing conditions (10, 39). Rajeeve et al. showed that *C. trachomatis* uses the chlamydial protease-like activating factor (CPAF) to inhibit neutrophil activation and cell death thereby creating a replicative environment (39). Since CPAF is highly conserved among chlamydiae, *C. pnuemoniae* may use a similar CPAF-dependent mechanism to survive and replicate in neutrophils.

Similarly, co-incubating monocytes and *C. pneumoniae* under non-opsonizing conditions leads to recovery of chlamydial progeny up until 48 hours post infection (9, 40) suggesting that opsonin-independent uptake also facilitates *C. pneumoniae* survival in monocytes. This idea was further supported by the observation that differentiated macrophages support intracellular replication of *C. pneumoniae*. Differentiated macrophages, but not peripheral blood monocytes, express the mannose receptor (MR) which facilitate intracellular survival of *M. tuberculosis*, and MR has also been linked to phagocytic uptake of chlamydial organisms (12, 41, 42). Others used commercially available human serum from AB blood type donors in the infection medium combined with centrifugation. These studies were unable to recover chlamydial progeny after 6 and 48 hours, but detected 16S rRNA suggesting metabolic, but not replicative activity (8, 43). However, neither complement functional activity nor serostatus were evaluated for these sera making it difficult to draw any conclusions on the role of opsonization. We demonstrated that both complement- and IgG-opsonization potentiates phagocytosis and intracellular killing of *C. pneumoniae* suggesting that the uptake mechanism is important for the intracellular fate of *C. pneumoniae* previously demonstrated for other chlamydial organisms (44).

Here we demonstrated that complement opsonization and to a lesser extend IgG opsonization inhibits *C. pneumoniae* progeny infection and facilitates *C. pneumoniae* uptake in human monocytes and neutrophils. Ingested bacteria are rapidly trafficked to destructive intracellular compartments and eliminated showing that opsonization and phagocytosis are efficient means of controlling extracellular *C. pneumoniae* organisms. Thus, opsonization is a critical factor to include in future *in vitro* studies exploring the interaction between *C. pneumoniae* and human phagocytes.

MATERIALS AND METHODS

Antibodies and reagents

The following primary antibodies were used in this study: PE anti-human CD14 (Clone: M5E2) (BioLegend, CA, USA), MAb 15.2.3 against chlamydial LPS (45), PAb198 against *C. pneumoniae* outer membrane (46), Anti-MRP8 (S100A8) (Abcam, UK), Anti-LAMP1 (Sino Biological, China), Polyclonal Rabbit Anti-Human C3c (Agilent Technologies, Glostrup, Denmark), Polyclonal Rabbit Anti-Human C4c (Agilent) and Monoclonal Mouse Anti-Human C5b-9 (clone aE11, Agilent).

The following secondary antibodies were used in this study: Goat anti human IgG-, Goat anti rabbit and Goat anti mouse antibody conjugated to 10 nm colloidal gold (British BioCell, Cardiff, UK) was used for immunoelectron microscopy. Horseradish peroxidase conjugated Affinipure Goat Anti-Human Fcγ-specific IgG was used for ELISA. Anti-Rabbit IgG conjugated to alkaline phosphatase was used for western blotting (Sigma Aldrich, MO, USA). FITC-conjugated Goat Anti-Human IgG, Fcγ fragment specific (Jackson ImmunoResearch, Cambridge, UK), Alexa Fluor® (AF) 555 goat anti-rabbit, AF555 goat anti-mouse and AF647 goat anti-rabbit (Invitrogen, Thermo Fisher Scientific, MA, USA) were used for immunofluorescence staining.

TMB/ONE (3,3’,5, 5’-tetramethylbenzidine) and BCIP/NBT (5-bromo-4-chloro-3-indolyl phosphate/ Nitro Blue Tetrazolium) were purchased from Kementec (Kementec, Taastrup, Denmark) and used for ELISA and western blotting, respectively.

Cell lines and culture

BHK- and HeLa cell lines were purchased from the American Type Culture Collection (ATCC, VA, USA) and cultured in complete medium consisting of RPMI 1640 supplemented with 5% fetal calf serum (FCS), and 0.01 mg/ml gentamicin and maintained at 37°C and 5% CO_2. Cell lines were tested free of mycoplasma by Hoechst (33258) staining.

Bacterial organism and propagation

C. pneumoniae (CDC/CWL-029/VR1310) was purchased from ATCC and cultivated in Baby Hamster kidney (BHK) cells in complete medium added 2 µg/ml cycloheximide and 0.1% glucose. The infected cells were cultured at 37°C and 5% CO_2 for 72 hours. *C. pneumoniae* EBs were purified by density gradient centrifugation as previously described (46). Mock inoculum was prepared by processing uninfected BHK cells in parallel with infected cells.

Serum samples

Serum was obtained from 10 healthy volunteers at Aalborg University, Denmark. Blood was drawn by venipuncture and collected in S-Monovette® serum tubes (Sarstedt, Nümbrecht, Germany) and serum was isolated immediately according to manufactures instructions. Isolated serum was immediately stored on ice before freezing at -80 °C for later use. Serum heat inactivation was done for 30 min at 56°C. Serum containing anti-*C. pneumoniae* IgG is denoted "immune serum" and serum without anti-*C. pneumoniae* IgG is denoted "non-immune serum". Throughout this paper the following abbreviations will be used described the different sera: NHS+: Immune serum, NHS-: Non-immune serum, HIHS+: heat-inactivated immune serum and HIHS-: heat-inactivated non-immune serum.

All protocols were approved by the Regional ethics committee of Region Nordjylland (N-20150073) and all experiments were carried according to the Declaration of Helsinki. All participants gave written informed consent to participate in the study.

ELISA

C. pneumoniae specific IgG was measured using *Chlamydia pneumoniae*-IgG ELISA Medac plus (Medac, Wedel, Germany) using *C. pneumoniae* outer membrane complex as antigen. Absorbance were measured at 450 nm on a Sunrise™ microplate reader (Tecan, Mannedorf, Switzerland).

Immunofluorescence validation of serum reactivity

HeLa cell monolayers, seeded on coverslips, were infected with $5x10^5$ inclusion forming units (IFU) *C. pneumoniae* by centrifugation at 1000 x g for 30 min at 37°C followed by 30 min incubation at 37°C and 5% CO_2. Medium containing extracellular bacteria was removed and cells were incubated in complete medium added 2 µg/ml cycloheximide and 0.1% glucose for 48 hours and subsequently fixed in 3.7% formaldehyde for 20 min at 4 °C. Cells were permeabilized in ice cold methanol for 10 min, blocked in 0.5% bovine serum albumin (BSA) for 15 min at 37°C and incubated with serial dilutions of immune- and non-immune serum for 30 min at 37°C. Cells were washed three times in PBS and incubated with FITC-conjugated anti-human IgG secondary antibody diluted 1:200 in 0.1% BSA in PBS for 30 min at 37°C. Cells were washed three times in PBS and counter stained with using 2 µM

To-Pro-3 Iodide (Invitrogen, Thermo Fisher Scientific) for 20 min at room temperature. Cells were imaged using a Leica TCS SP5 confocal laser scanning microscope with a HCX PL Apo 63x/1.40 and CX PL Apo 100x/1.47 objective (Leica Microsystems, Wetzlar, Germany).

Immunogold-labeling and transmission electron microscopy (TEM)

Purified *C. pneumoniae* EBs were incubated in 50% NHS or HIHS for 30 min at 37°C and washed three times in PBS with centrifugation at 15.000 x g, for 15 min at 4°C between each wash. Processing and immunogold-labeling of bacteria for TEM was performed as previously described (47). Briefly, serum coated (NHS or HIHS) *C. pneumoniae* EBs were added to carbon coated 400-mesh glow-discharged nickel grids and washed three times in PBS before blocking in 1% ovalbumin (Sigma-Aldrich) in PBS (pH 6.5). To determine binding of human antibodies to the chlamydial surface, grids were incubated for 30 min at 37°C with Goat anti human IgG conjugated to 10 nm colloidal gold diluted 1:25 in 0.5% ovalbumin in PBS. To determine complement binding. samples were incubated with primary antibodies (anti-C3c, 1:200; anti-C4c, 1:200; anti-C5b-9, 1:20) diluted in 0.5% ovalbumin in PBS for 30 min at 37°C. Grids were washed in three drops of PBS and subsequently incubated for 30 min at 37°C with secondary antibodies (Goat anti rabbit or Goat anti mouse antibody conjugated to 10 nm colloidal gold) diluted 1:25 in 0.5% ovalbumin in PBS. The grids were washed in three drops PBS, incubated in three drops of 0.5% cold fish gelatin in PBS and negatively stained with 0.5% phosphotungstic acid (PTA). Grids were blotted dry on filter paper and investigated using a Jeol 1010 transmission electron microscope (Jeol, Tokyo, Japan). Gold-deposition was quantified as previously described (47). Briefly, a minimum of seven random fields were imaged for each grid containing at least 12 chlamydial organisms in total. For each chlamydial organism, gold particles on the bacteria and in the background were counted and the density of deposition was calculated for both (gold per area). From these numbers, a bacteria-to-background ratio was calculated to quantitatively describe bacterial gold deposition relative to background deposition. From these ratios the median and interquartile ranges (IQR) were calculated for each sample.

Western blotting

SDS-PAGE and western blotting were performed essentially according to Lausen et al. (47). Briefly, purified *C. pneumoniae* EBs were incubated in 50% serum for 30 minutes at 37°C and unbound complement was removed by washing three times in PBS with centrifugation at 15,000 x g for 15 min between each wash. The chlamydial pellet was lysed in SDS Sample buffer + 5% β-mercaptoethanol and proteins were separated on an 8 % polyacrylamide gel. Proteins were blotted on to a nitrocellulose membrane (GE Healthcare Life Sciences IL, USA) in Tris-Glycine buffer (25 mM Tris, 192mM glycine) + 20% methanol for two hours at 100 V using a TE22 Mighty Small Transfer Tank (Hoefer, Inc., Holliston, MA).

Membranes were blocked for 30 min at 37°C in 3% gelatin in Tris-buffered saline (TBS). Antibodies diluted in TBS + 0.05% Tween-20 (TBST) + 0.2% gelatin were added to the membranes and left for incubation for one hour at 37°C. Blots were washed three times in TBST and incubated with alkaline phosphatase-conjugated secondary antibody for one hour at 37°C. Antigen-antibody complexes were visualized by adding BCIP/NBT (Kementec) alkaline phosphatase substrate.

Serum neutralization assay

C. pneumoniae EBs were incubated in RPMI 1640 supplemented with 10% human serum for 30 min at 37°C. Opsonized bacteria (10.8x10^4 IFU for NHS samples and 1.2x10^4 IFU for HIHS samples) were used to infect HeLa cell monolayers as described above. Cells were processed for immunofluorescence microscopy as described above with minor modifications. PAb198 (1:400) and FITC-conjugated goat anti-rabbit (1:200) were used as primary and secondary antibodies, respectively, and cell nuclei were stained with 2 µg/ml DAPI.

The cells were inspected using a Leica LSM550 fluorescence microscope and images were captured from seven random fields in each sample. All samples were analyzed in duplicates and repeated in three independent experiments. The number of IFU was enumerated and expressed as percentage of initial inoculum. Data from the three experiments are expressed as mean ± standard deviation (SD).

FITC-labelling of bacteria

C. pneumoniae inoculum was suspended in 0.1 M $NaHCO_3$ (pH = 9) and centrifuged for 15 min at 15.000 x g. Fluorescein isothiocyanate isomer 1 (FITC) (Sigma, MO, USA) was added at a concentration of 0.1 mg/ml in 0.1 M $NaHCO_3$ buffer and bacteria were incubated for one hour protected from light. The labeled bacteria were washed three times in PBS to remove unbound FITC and the final bacteria pellet was suspended in sucrose-phosphate buffer (2SP), aliquoted, and stored at -80°C.

Immune cell isolation and culture

Peripheral blood was obtained from two donors (one seropositve and one seronegative) and collected in S-Monovette (Sarstedt) EDTA tubes. Blood was layered on Polymorphprep™ density gradient medium (Axis-Shield, Dundee, UK) and centrifuged for 40 min at 300 x g at 20°C. Layers with peripheral blood mononuclear cells (PBMCs) and polymorphnuclear cells were harvested and collected in the same tube when used for flow cytometry. The two cell populations were kept separate when used for immunofluorescence microscopy. Platelets was removed by centrifugation at 120 x g for 10 min at 20°C. Cells were resuspended in complete RPMI 1640 medium.

Immunofluorescence staining and microscopy of immune cells

For immunofluorescence staining, PBMCs were seeded in 8-well Nunc® Lab-Tek® Chamber™ slides with a density of 9 x 10^5 cells/well. Cells were left to adhere for 90 min and non-adherent cells were removed by washing twice in PBS. Bacteria were added at a multiplicity of infection (MOI) 10 in RPMI 1640 + 10% human serum.

Non-phagocytized bacteria were removed by washing three times in PBS and cells were processed for immunofluorescence staining as described above. PAb198 (1:400), anti-LAMP1 (1:400), anti-S100A8 (1:300) and MAb 15.2.3 (1:20) were used as primary antibodies and AF555-conjugated goat anti-mouse, AF555-conjugated goat anti-rabbit and AF647-conjugated goat anti-rabbit were used as secondary antibodies in an 1:200 dilution. Cell nuclei were stained using 2 µM To-Pro-3 Iodide (Invitrogen, Thermo Fisher Scientific). Cells were imaged using a Leica TCS SP5 confocal laser scanning microscope with a CX PL Apo 100x/1,47 objective (Leica Microsystems).

Phagocytosis assay

FITC-labeled *C. pneumoniae* EBs were opsonized in RPMI 1640 + 10% human serum for 15 min at 37°C. Bacteria ($1x10^7$ or $1x10^6$ bacteria/tube) and immune cells ($1x10^6$ cells/tube) were mixed in 5 ml polypropylene tubes (MOI=10 and MOI=1, respectively) and co-incubated for 30 min at 37°C and cells were subsequently processed for flow cytometry.

Flow cytometry

Cells were washed in cold PBS + 0.05% sodium azide to remove non-phagocytized bacteria. Fc-receptors were blocked using 20 µg/ml human IgG (Sigma) for 15 min at 4°C. Primary fluorochrome-conjugated antibodies, diluted in PBS + 0.05% sodium azide + 0.01% BSA, were added and cells were stained for 30 min at room temperature. Unbound antibody was removed by washing in PBS and cell viability was assessed using eBioscience™ Fixable Viability dye eFluor™ 450 according to manufacturers's instructions. The cells were washed twice in PBS and fixed in 1% formaldehyde for 20 min at 4°C and analyzed on a CytoFLEX flow cytometer (Beckman Coulter, CA, USA).

IgG purification

Serum from one seropositive donor was mixed 1:1 with binding buffer (1 M glycine, 150 mM NaCl, pH 8.5) and the serum IgG fraction was isolated on an affinity chromatography column packed with

GammaBind Plus protein G Sepharose (GE Healthcare). Bound IgG was eluted from the column using elution buffer containing 100 mM glycine-HCl pH 2.7 and collected in 25 fractions in tubes containing 1 M Tris-HCl pH 9 to restore neutral pH. The protein concentration in each fraction was determined using Pierce™ BCA Protein Assay Kit (Thermo Scientific) according to manufacturer's instruction.

Intracellular survival assay

PBMCs and neutrophils were co-incubated with bacteria as described above. Cells were washed three times in PBS to remove non-phagocytized bacteria. The cell pellet was suspended in 2SP buffer and cells were lysed by ultrasonication to liberate ingested bacteria. The cell lysates were used to infect HeLa cells and IFU were quantified from duplicate samples in three independent experiments as described above.

Data analysis

Flow cytometry data were analyzed using FlowLogic™ v.7.2.1 (Inivai Technologies, Mentone Victoria, Australia). One-way ANOVA with Tukey's post hoc or Welch ANOVA with Games-Howell multiple comparison test was used to investigate differences between multiple means. Differences between means from two independent groups were investigated using student's independent t-test or Welch's t-test. All statistical analyses were performed in SPSS Statistics 25 (IBM, Armonk, NY, USA).

ACKNOWLEDGEMENTS

We would like to thank Ditte Bech Laursen for technical assistance. This study was funded by Aase and Ejner Danielsen foundation, the Obel Family Foundation and by the Joint Strategic Research Programme on Fighting antibiotic Resistance (Aalborg University and University of Southern Denmark)

CONFLICT OF INTEREST

The authors declare no conflict of interest.

REFERENCES

1. **Porritt RA**, **Crother TR**. 2017. Chlamydia pneumoniae Infection and Inflammatory Diseases. For Immunopathol Dis Therap **7**:237–254.

2. **Grayston JT**, **Belland RJ**, **Byrne GI**, **Kuo CC**, **Schachter J**, **Stamm WE**, **Zhong G**. 2015. Infection with Chlamydia pneumoniae as a cause of coronary heart disease: the hypothesis is still untested. Pathog Dis **73**:1–9.

3. **Elwell C**, **Mirrashidi K**, **Engel J**. 2016. Chlamydia cell biology and pathogenesis. Nat Rev Microbiol **14**:385–400.

4. **Zuck M**, **Sherrid A**, **Suchland R**, **Ellis T**, **Hybiske K**. 2016. Conservation of extrusion as an exit mechanism for Chlamydia. Pathog Dis **74**:ftw093.

5. **Jahn H**, **Krüll M**, **Wuppermann FN**, **Klucken AC**, **Rosseau S**, **Seybold J**, **Hegemann JH**, **Jantos CA**, **Suttorp N**. 2000. Infection and Activation of Airway Epithelial Cells by *Chlamydia pneumoniae*. J Infect Dis **182**:1678–1687.

6. **Gieffers J**, **van Zandbergen G**, **Rupp J**, **Sayk F**, **Krüger S**, **Ehlers S**, **Solbach W**, **Maass M**. 2004. Phagocytes transmit Chlamydia pneumoniae from the lungs to the vasculature. Eur Respir J **23**:506–510.

7. **Chiba N**, **Shimada K**, **Chen S**, **Jones HD**, **Alsabeh R**, **Slepenkin A V**, **Peterson E**, **Crother TR**, **Arditi M**. 2015. Mast cells play an important role in chlamydia pneumoniae lung infection by facilitating immune cell recruitment into the airway. J

Immunol **194**:3840–51.

8. **Buchacher T**, **Wiesinger-Mayr H**, **Vierlinger K**, **Rüger BM**, **Stanek G**, **Fischer MB**, **Weber V**. 2014. Human blood monocytes support persistence, but not replication of the intracellular pathogen C. pneumoniae. BMC Immunol **15**:60.

9. **Marangoni A**, **Bergamini C**, **Fato R**, **Cavallini C**, **Donati M**, **Nardini P**, **Foschi C**, **Cevenini R**. 2014. Infection of human monocytes by Chlamydia pneumoniae and Chlamydia trachomatis: an in vitro comparative study. BMC Res Notes **7**:230.

10. **van Zandbergen G**, **Gieffers J**, **Kothe H**, **Rupp J**, **Bollinger A**, **Aga E**, **Klinger M**, **Brade H**, **Dalhoff K**, **Maass M**, **Solbach W**, **Laskay T**. 2004. *Chlamydia pneumoniae* Multiply in Neutrophil Granulocytes and Delay Their Spontaneous Apoptosis. J Immunol **172**:1768–1776.

11. **Schlesinger LS**. 1996. Entry of Mycobacterium tuberculosis into mononuclear phagocytes. Curr Top Microbiol Immunol **215**:71–96.

12. **Kang PB**, **Azad AK**, **Torrelles JB**, **Kaufman TM**, **Beharka A**, **Tibesar E**, **DesJardin LE**, **Schlesinger LS**. 2005. The human macrophage mannose receptor directs Mycobacterium tuberculosis lipoarabinomannan-mediated phagosome biogenesis. J Exp Med **202**:987–99.

13. **Jensen TS**, **Opstrup K V.**, **Christiansen G**, **Rasmussen P V.**, **Thomsen ME**, **Justesen DL**, **Schønheyder HC**, **Lausen M**, **Birkelund S**. 2020. Complement mediated

Klebsiella pneumoniae capsule changes. Microbes Infect **22**:19–30.

14. **Merle NS**, **Church SE**, **Fremeaux-Bacchi V**, **Roumenina LT**. 2015. Complement System Part I - Molecular Mechanisms of Activation and Regulation. Front Immunol **6**:262.

15. **Ferguson JS**, **Weis JJ**, **Martin JL**, **Schlesinger LS**. 2004. Complement protein C3 binding to Mycobacterium tuberculosis is initiated by the classical pathway in human bronchoalveolar lavage fluid. Infect Immun **72**:2564–2573.

16. **Bolger MS**, **Ross DAS**, **Jiang H**, **Frank MM**, **Ghio AJ**, **Schwartz DA**, **Wright JR**. 2007. Complement levels and activity in the normal and LPS-injured lung. Am J Physiol - Lung Cell Mol Physiol **292**:748–759.

17. **Gaede KI**, **Wilke G**, **Brade L**, **Brade H**, **Schlaak M**, **Müller-Quernheim J**. 2002. Anti-Chlamydophila immunoglobulin prevalence in sarcoidosis and usual interstitial pneumoniae. Eur Respir J **19**:267–274.

18. **Cortes C**, **Ferreira VP**, **Pangburn MK**. 2011. Native properdin binds to Chlamydia pneumoniae and promotes complement activation. Infect Immun **79**:724–731.

19. **Kihlström E**, **Majeed M**, **Rozalska B**, **Wadström T**. 1992. Binding of Chlamydia trachomatis serovar L2 to collagen types I and IV, fibronectin, heparan sulphate, laminin and vitronectin. Zentralbl Bakteriol **277**:329–33.

20. **Swanson AF**, **Kuo CC**. 1990. Identification of lectin-binding proteins in Chlamydia

species. Infect Immun **58**:502–7.

21. **Swanson AF**, **Ezekowitz RA**, **Lee A**, **Kuo CC**. 1998. Human mannose-binding protein inhibits infection of HeLa cells by Chlamydia trachomatis. Infect Immun **66**:1607–12.

22. **Hjelholt A**, **Christiansen G**, **Sørensen US**, **Birkelund S**. 2013. IgG subclass profiles in normal human sera of antibodies specific to five kinds of microbial antigens. Pathog Dis **67**:206–213.

23. **Su H**, **Spangrude GJ**, **Caldwell HD**. 1991. Expression of FcγRIII on HeLa 229 cells: Possible effect on in vitro neutralization of Chlamydia trachomatis. Infect Immun. American Society for Microbiology (ASM).

24. **Scidmore MA**, **Rockey DD**, **Fischer ER**, **Heinzen RA**, **Hackstadt T**. 1996. Vesicular interactions of the Chlamydia trachomatis inclusion are determined by chlamydial early protein synthesis rather than route of entry. Infect Immun **64**:5366–5372.

25. **Gigli I**, **Fujita T**, **Nussenzweig V**. 1979. Modulation of the classical pathway C3 convertase by plasma proteins C4 binding protein and C3b inactivator. Proc Natl Acad Sci **76**:6596–6600.

26. **Berggard K**, **Johnsson E**, **Morfeldt E**, **Persson J**, **Stalhammar-Carlemalm M**, **Lindahl G**. 2001. Binding of human C4BP to the hypervariable region of M protein: a molecular mechanism of phagocytosis resistance in Streptococcus pyogenes. Mol Microbiol **42**:539–551.

27. **Prasadarao N V.**, **Blom AM**, **Villoutreix BO**, **Linsangan LC**. 2002. A Novel Interaction of Outer Membrane Protein A with C4b Binding Protein Mediates Serum Resistance of *Escherichia coli* K1. J Immunol **169**:6352–6360.

28. **Watford WT**, **Ghio AJ**, **Wright JR**. 2000. Complement-mediated host defense in the lung. Am J Physiol Lung Cell Mol Physiol **279**:L790-8.

29. **Geier H**, **Celli J**. 2011. Phagocytic Receptors Dictate Phagosomal Escape and Intracellular Proliferation of Francisella tularensis. Infect Immun **79**:2204–2214.

30. **Bode J**, **Dutow P**, **Sommer K**, **Janik K**, **Glage S**, **Tummler B**, **Munder A**, **Laudeley R**, **Sachse KW**, **Klos A**. 2012. A new role of the complement system: C3 provides protection in a mouse model of lung infection with intracellular Chlamydia psittaci. PLoS One **7**:e50327.

31. **Dutow P**, **Fehlhaber B**, **Bode J**, **Laudeley R**, **Rheinheimer C**, **Glage S**, **Wetsel RA**, **Pabst O**, **Klos A**. 2014. The Complement C3a Receptor Is Critical in Defense against Chlamydia psittaci in Mouse Lung Infection and Required for Antibody and Optimal T Cell Response. J Infect Dis **209**:1269–1278.

32. **Martin U**, **Bock D**, **Arseniev L**, **Tornetta MA**, **Ames RS**, **Bautsch W**, **Köhl J**, **Ganser A**, **Klos A**. 1997. The human C3a receptor is expressed on neutrophils and monocytes, but not on B or T lymphocytes. J Exp Med **186**:199–207.

33. **Chenoweth DE**, **Hugli TE**. 1978. Demonstration of specific C5a receptor on intact

human polymorphonuclear leukocytes. Proc Natl Acad Sci U S A **75**:3943–3947.

34. **Brekke O-L**, **Christiansen D**, **Fure H**, **Fung M**, **Mollnes TE**. 2007. The role of complement C3 opsonization, C5a receptor, and CD14 in E. coli-induced up-regulation of granulocyte and monocyte CD11b/CD18 (CR3), phagocytosis, and oxidative burst in human whole blood. J Leukoc Biol **81**:1404–1413.

35. **Mollnes TE**, **Brekke O-L**, **Fung M**, **Fure H**, **Christiansen D**, **Bergseth G**, **Videm V**, **Lappegard KT**, **Kohl J**, **Lambris JD**. 2002. Essential role of the C5a receptor in E coli-induced oxidative burst and phagocytosis revealed by a novel lepirudin-based human whole blood model of inflammation. Blood **100**:1869–1877.

36. **Sengeløv H**, **Kjeldsen L**, **Kroeze W**, **Berger M**, **Borregaard N**. 1994. Secretory vesicles are the intracellular reservoir of complement receptor 1 in human neutrophils. J Immunol **153**:804–10.

37. **Crowell RE**, **Van Epps DE**. 1990. Nonsteroidal antiinflammatory agents inhibit upregulation of CD11b, CD11c, and CD35 in neutrophils stimulated by formyl-methionine-Leucine-phenylalanine. Inflammation **14**:163–171.

38. **Furtado PB**, **Huang CY**, **Ihyembe D**, **Hammond RA**, **Marsh HC**, **Perkins SJ**. 2008. The Partly Folded Back Solution Structure Arrangement of the 30 SCR Domains in Human Complement Receptor Type 1 (CR1) Permits Access to its C3b and C4b Ligands. J Mol Biol **375**:102–118.

39. **Rajeeve K**, **Das S**, **Prusty BK**, **Rudel T**. 2018. Chlamydia trachomatis paralyses neutrophils to evade the host innate immune response. Nat Microbiol **3**:824–835.

40. **Wolf K**, **Fischer E**, **Hackstadt T**. 2005. Degradation of Chlamydia pneumoniae by peripheral blood monocytic cells. Infect Immun **73**:4560–70.

41. **Martinez-Pomares L**. 2012. The mannose receptor. J Leukoc Biol **92**:1177–1186.

42. **Lausen M**, **Christiansen G**, **Bouet Guldbæk Poulsen T**, **Birkelund S**. 2019. Immunobiology of monocytes and macrophages during Chlamydia trachomatis infection. Microbes Infect **21**:73–84.

43. **Airenne S**, **Surcel HM**, **Alakärppä H**, **Laitinen K**, **Paavonen J**, **Saikku P**, **Laurila A**. 1999. Chlamydia pneumoniae infection in human monocytes. Infect Immun **67**:1445–1449.

44. **Prain CJ**, **Pearce JH**. 1989. Ultrastructural studies on the intracellular fate of Chlamydia psittaci (strain guinea pig inclusion conjunctivitis) and Chlamydia trachomatis (strain lymphogranuloma venereum 434): modulation of intracellular events and relationship with endocytic mechan. J Gen Microbiol **135**:2107–23.

45. **Birkelund S**, **Lundemose AG**, **Christiansen G**. 1988. Chemical cross-linking of Chlamydia trachomatis. Infect Immun **56**:654–659.

46. **Knudsen K**, **Madsen AS**, **Mygind P**, **Christiansen G**, **Birkelund S**. 1999. Identification of two novel genes encoding 97- to 99-kilodalton outer membrane proteins

of Chlamydia pneumoniae. Infect Immun **67**:375–83.

47. **Lausen M**, **Christiansen G**, **Karred N**, **Winther R**, **Poulsen TBG**, **Palarasah Y**, **Birkelund S**. 2018. Complement C3 opsonization of Chlamydia trachomatis facilitates uptake in human monocytes. Microbes Infect **20**:328–336.

FIGURE LEGENDS

Figure 1

Complement opsonization of *C. pneumoniae* in non-immune serum. Purified *C. pneumoniae* EBs were incubated in A) non-immune serum (NHS-) or B) heat-inactivated non-immune serum (HIHS-) and analyzed by immunoelectron microscopy (IEM) using anti-C3c and anti-rabbit 10 nm colloidal gold as primary and secondary antibodies, respectively. C) Gold deposition on each bacterium was quantified relative to the background gold level for each condition (NHS- and HIHS-). D) Purified *C. pneumoniae* EBs were subjected to western blot analysis and labeled against C3c. *C. pneumoniae* EBs were incubated in E) NHS- or F) HIHS- and subjected to IEM using anti-C4c as primary antibody. G) Complement C4 deposition was quantified as described for panel C). H) Western blot analysis of complement C4 deposition on *C. pneumoniae* incubated in NHS- or HIHS-. Western blot analysis was repeated three times and representative blots are shown. IEM images were captured from at least 8 random fields for each sample in one experiment. For each bacterium, a bacterium-to-background gold deposition ratio was calculated and plotted with each dot representing one chlamydial organism. The median ratio is presented as black lines. Scale bars indicate 200 nm.

Figure 2

Antibody- and complement opsonization of *C. pneumoniae* in immune serum. *C. pneumoniae* ($5x10^5$ IFU/well) were grown in in HeLa cells for 48 hours and chlamydial inclusions were immunofluorescently stained using two-fold serial dilutions of A) immune serum or B) non-immune serum as primary antibody. Purified *C. pneumoniae* EBs incubated in C) heat-inactivated immune serum (HIHS+) or D) heat-inactivated non-immune serum (HIHS-) were immuno-labeled with anti-human IgG 10 nm colloidal gold and subjected to immuno-electron microscopy (IEM). E) From IEM images, chlamydial gold deposition, for each bacterium, was quantified relative to the background gold level. Purified *C. pneumoniae* EBs were incubated in F) immune serum (NHS+) or G) heat-inactivated immune serum (HIHS+) and analyzed by IEM using anti-C3c and anti-rabbit 10 nm colloidal gold as primary and secondary antibodies, respectively. H) Gold deposition in IEM images was quantified as described for panel E. I) Purified *C. pneumoniae* EBs were subjected to western blot analysis and labeled against C3c. J-M) *C. pneumoniae* were treated as described in panel F-I except bacteria were labeled using an anti-C4c antibody. For immunofluorescence microcopy, each serum was tested in four different dilutions and images were captured from five random fields for each dilution. The experiment was repeated twice. In IEM, a bacterium-to-background gold deposition ratio was calculated for each bacterium and plotted, with each dot representing one chlamydial organism. The median ratio is presented as black lines. IEM images were captured from at least 8 random fields for each sample in one experiment. Western blot analysis was repeated three times and representative blots are shown. Scale bars indicate 10 µm (A,B) and 200 nm (C,D,F,G,J,K).

Figure 3

Formation of membrane attack complex (MAC) on *C. pneumoniae*. Purified *C. pneumoniae* EBs were incubated in immune- and non-immune serum and processed for IEM. Images show A) *C. pneumoniae* incubated in immune-serum (NHS+) and negatively stained with PTA. B) *C. pneumoniae* incubated in immune-serum (NHS+) and negatively stained with PTA and C) *C. pneumoniae* incubated in non-immune serum (NHS-) and immuno-gold labeled against C5b-9. Area with disintegrated bacterial morphology was enlarged (hatched boxes) demonstrating 10 nm pore-like structures (yellow arrowheads) (B+C) in close proximity to gold particles (C). D) *C. pneumoniae* incubated in heat-inactivated immune-serum (HIHS+) and immuno-gold labeled against C5b-9. Anti-mouse 10 nm colloidal gold was used as secondary antibody.

IEM images were used to quantify gold deposition on *C. pneumoniae* incubated in E) non-immune serum and F) immune serum. For each chlamydial organism, the gold particle deposition was quantified by calculating a bacteria-to-background ratio and the ratios were used to create scatter plots. Each dot represents the ratio from one chlamydial organism and the black lines show the median ratio. Scalebars indicate 200 nm. HIHS-: heat-inactivated non-immune serum.

Figure 4

Serum neutralization of *C. pneumoniae* EBs. *C. pneumoniae* inoculum were incubated in immune-serum (NHS+), non-immune serum (NHS-), heat-inactivated immune-serum (HIHS+), heat-inactivated non-immune serum (HIHS-) or HIHS- supplemented with 1.5 mg/ml IgG from immune-serum (HIHS-+IgG) for 30 min and used to infect HeLa cells. HeLa cells were inoculated with 10.8×10^4 inclusion forming units (IFU) of NHS-opsonized *C. pneumoniae* and 1.2×10^4 IFU of HIHS-opsonized *C. pneumoniae*. IFU were quantified by immunofluorescence staining of chlamydial inclusions. Images were captured from seven random fields in each sample using a 16X objective. Data were obtained from duplicate samples from three independent experiments. All data are presented as mean ± SD. Differences between means were analyzed by Welch's ANOVA with Games-Howell multiple comparisons test. P-values < 0.05 were considered statistically significant and denoted with an asterix (*).

Figure 5

Opsonophagocytosis of *C. pneumoniae* in monocytes and neutrophils. The percentage of *C. pneumoniae*-positive A) monocytes and B) neutrophils incubated with *C. pneumoniae* at MOI=10 in non-immune serum was quantified by flow cytometry. The combined role of complement and anti-*C. pneumoniae* IgG in C) monocyte and D) neutrophil phagocytosis was tested using immune serum. Heat-inactivated non-immune serum and heat-inactivated non-immune serum supplemented with the IgG fraction from immune serum was used as control to determine the role of IgG in phagocytosis in E) monocytes and F) neutrophils. The percentage of *C. pneumoniae*-positive G) monocytes and H) neutrophils incubated with *C. pneumoniae* at MOI=1 in immune serum and non-immune serum. Data were obtained from duplicate samples from three independent experiments except for E) + F) which was obtained from duplicate samples from two independent experiments. A minimum of 8,000 gated events were obtained from each sample. All data are presented as mean ± SD. One-way ANOVA with Tukey's post hoc test, Welch's ANOVA with Games-Howell multiple comparison test or Welch's t-test were used to compare column means. P-values < 0.05 were considered statistically significant and denoted with an asterix (*).

NHS+: Immune serum, NHS-: Non-immune serum, HIHS+: heat-inactivated immune serum, HIHS-: heat-inactivated non-immune serum, HIHS-+ IgG: heat-inactivated non-immune serum supplemented with IgG fraction from immune serum.

Figure 6

Intracellular neutralization of opsonized *C. pneumoniae* in PBMCs and neutrophils. *C. pneumoniae* (MOI=10) were incubated with A) PBMCs and B) neutrophils under different culture conditions for 30 min and cell lysates were prepared by ultrasonication. Lysates were used to infect HeLa cell monolayers and inclusion forming units (IFU) was enumerated after 48 hours by immunofluorescence microscopy. Intracellular localization of *C. pneumoniae* in monocytes after 30 min was investigated by immunofluorescence staining and confocal microscopy of C) *C. pneumoniae* and D) LAMP1. Frame E) shows an overlay image. F) Monocyte incubated with mock control. Confocal microscopy was repeated twice for all four (NHS+/NHS-/HIHS+/HIHS-) conditions and images were captured from five random fields in each sample.

Quantitative data were obtained from duplicate samples from three independent experiments. Data are presented as mean ± SD. Differences between means were analyzed by Welch's ANOVA with Games-Howell multiple comparisons test. P-values < 0.05 were considered statistically significant and denoted with an asterix (*). Scale bar indicates 5 µm. NHS+: Immune serum, NHS-: Non-immune serum, HIHS+: heat-inactivated immune serum, HIHS-: heat-inactivated non-immune serum

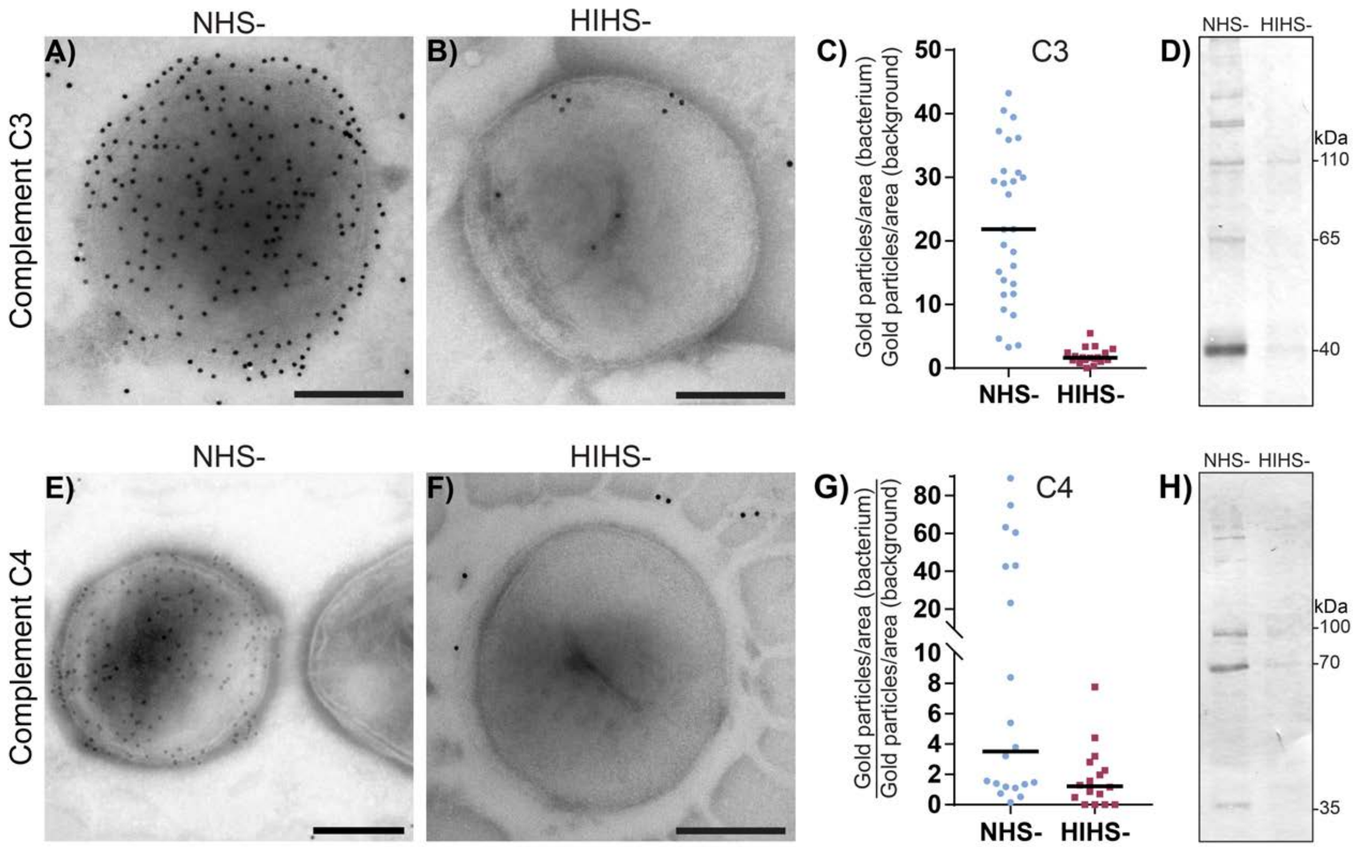
NHS-
HIHS-
Complement C3
A)
B)
C)
C3
Gold particles/area (bacterium)
Gold particles/area (background)
0
10
20
30
40
50
NHS-
HIHS-
D)
NHS-
HIHS-
kDa
-110
-65
-40
Complement C4
E)
F)
G)
C4
0
2
4
6
8
10
20
40
60
80
H)
kDa
-100
-70
-35

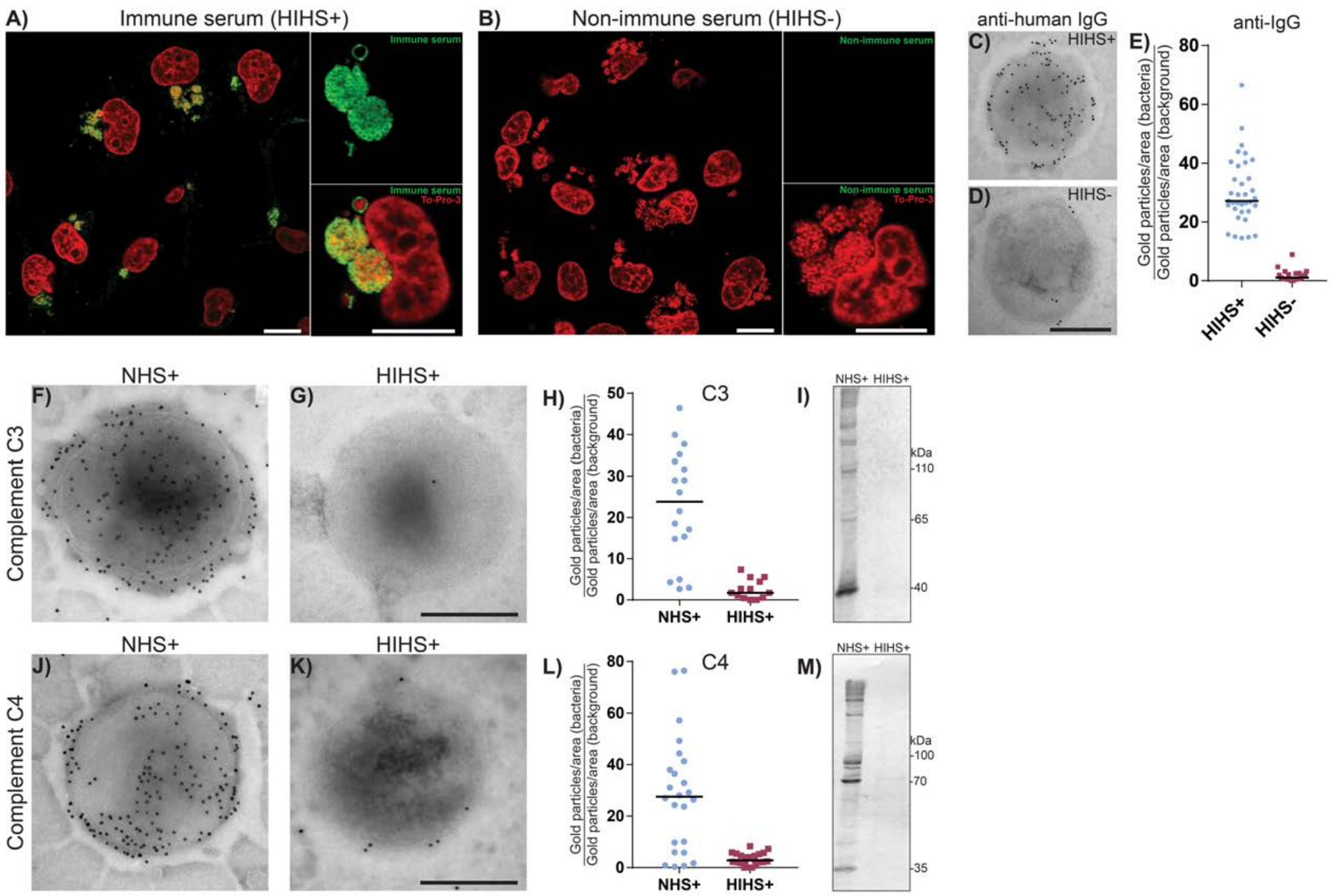
A) Immune serum (HIHS+)
Immune serum
Immune serum
To-Pro-3
B) Non-immune serum (HIHS-)
Non-immune serum
Non-immune serum
To-Pro-3
anti-human IgG
C) HIHS+
D) HIHS-
anti-IgG
E)
Gold particles/area (bacteria) / Gold particles/area (background)
80
60
40
20
0
HIHS+
HIHS-
NHS+
HIHS+
Complement C3
F)
G)
H) C3
50
40
30
20
10
0
NHS+
HIHS+
I)
NHS+ HIHS+
kDa
110
65
40
NHS+
HIHS+
Complement C4
J)
K)
L) C4
80
60
40
20
0
NHS+
HIHS+
M)
NHS+ HIHS+
kDa
100
70
35

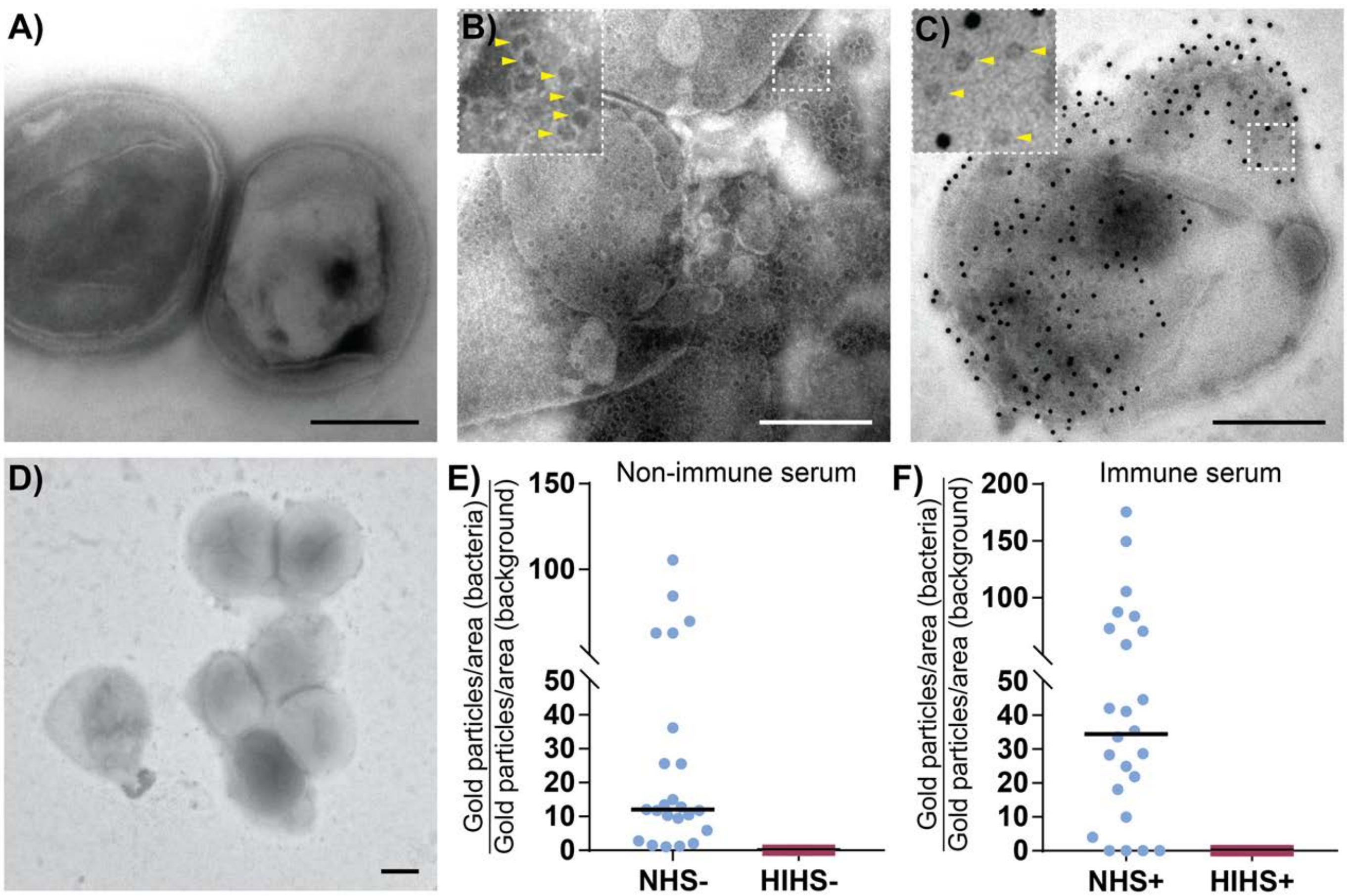
A)
B)
C)
D)
E)
Non-immune serum
Gold particles/area (bacteria) / Gold particles/area (background)
150
100
50
40
30
20
10
0
NHS-
HIHS-
F)
Immune serum
Gold particles/area (bacteria) / Gold particles/area (background)
200
150
100
50
40
30
20
10
0
NHS+
HIHS+

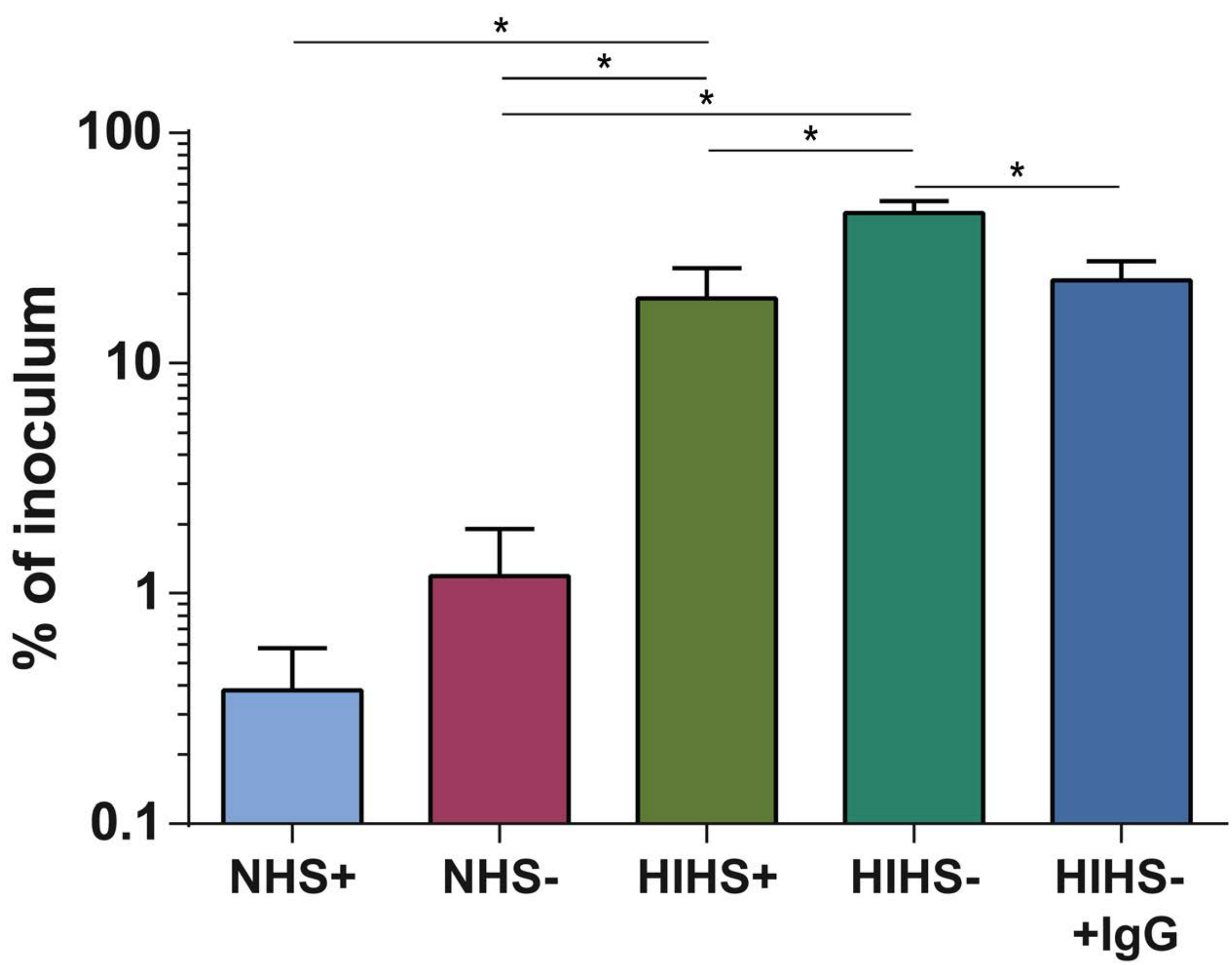
% of inoculum
100
10
1
0.1
*
*
*
*
*
NHS+
NHS-
HIHS+
HIHS-
HIHS-
+IgG

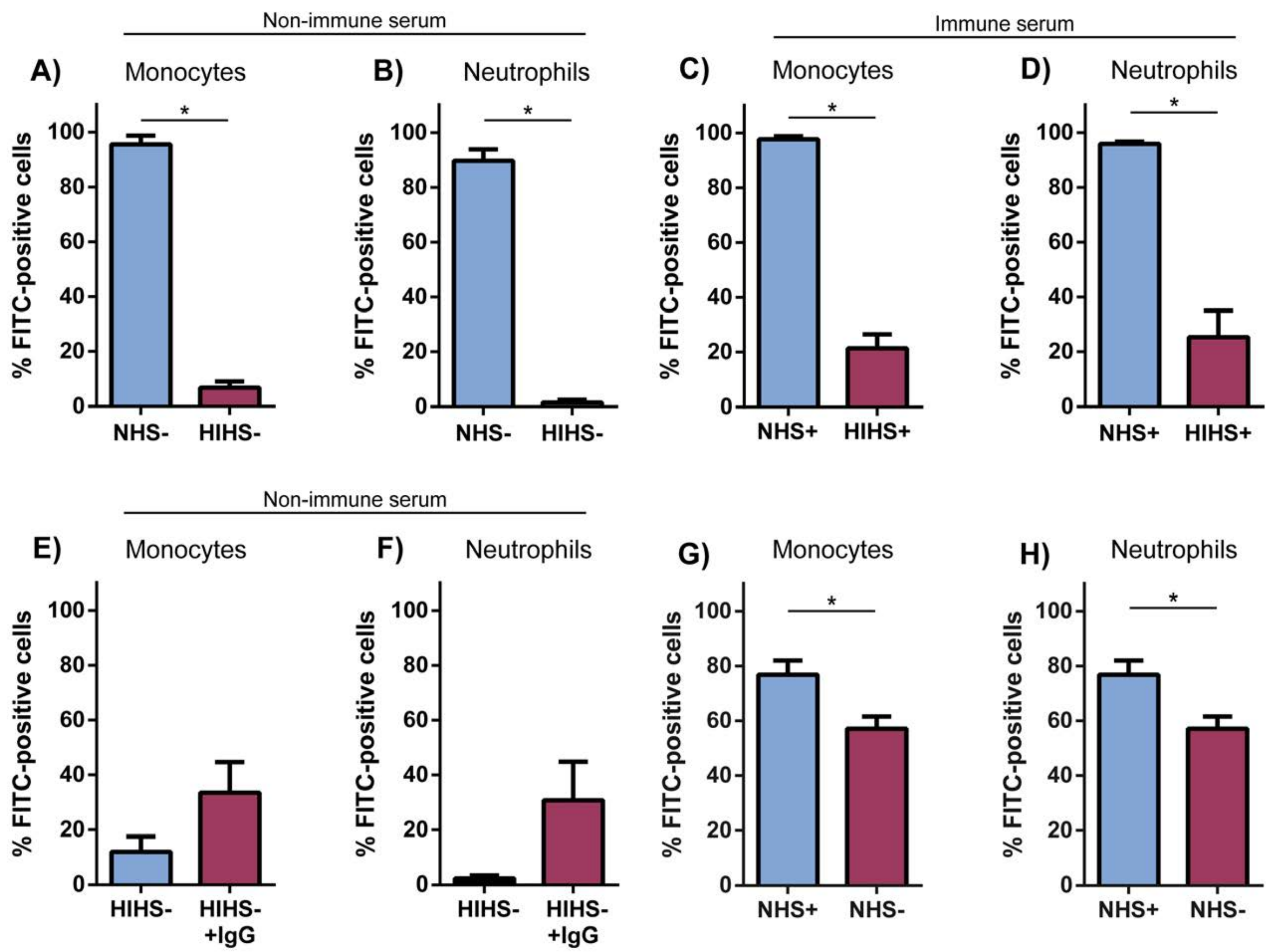
Non-immune serum
Immune serum
A) Monocytes
B) Neutrophils
C) Monocytes
D) Neutrophils
% FITC-positive cells
0
20
40
60
80
100
*
NHS-
HIHS-
NHS+
HIHS+
Non-immune serum
E) Monocytes
F) Neutrophils
G) Monocytes
H) Neutrophils
HIHS-
HIHS-
+IgG
NHS+
NHS-

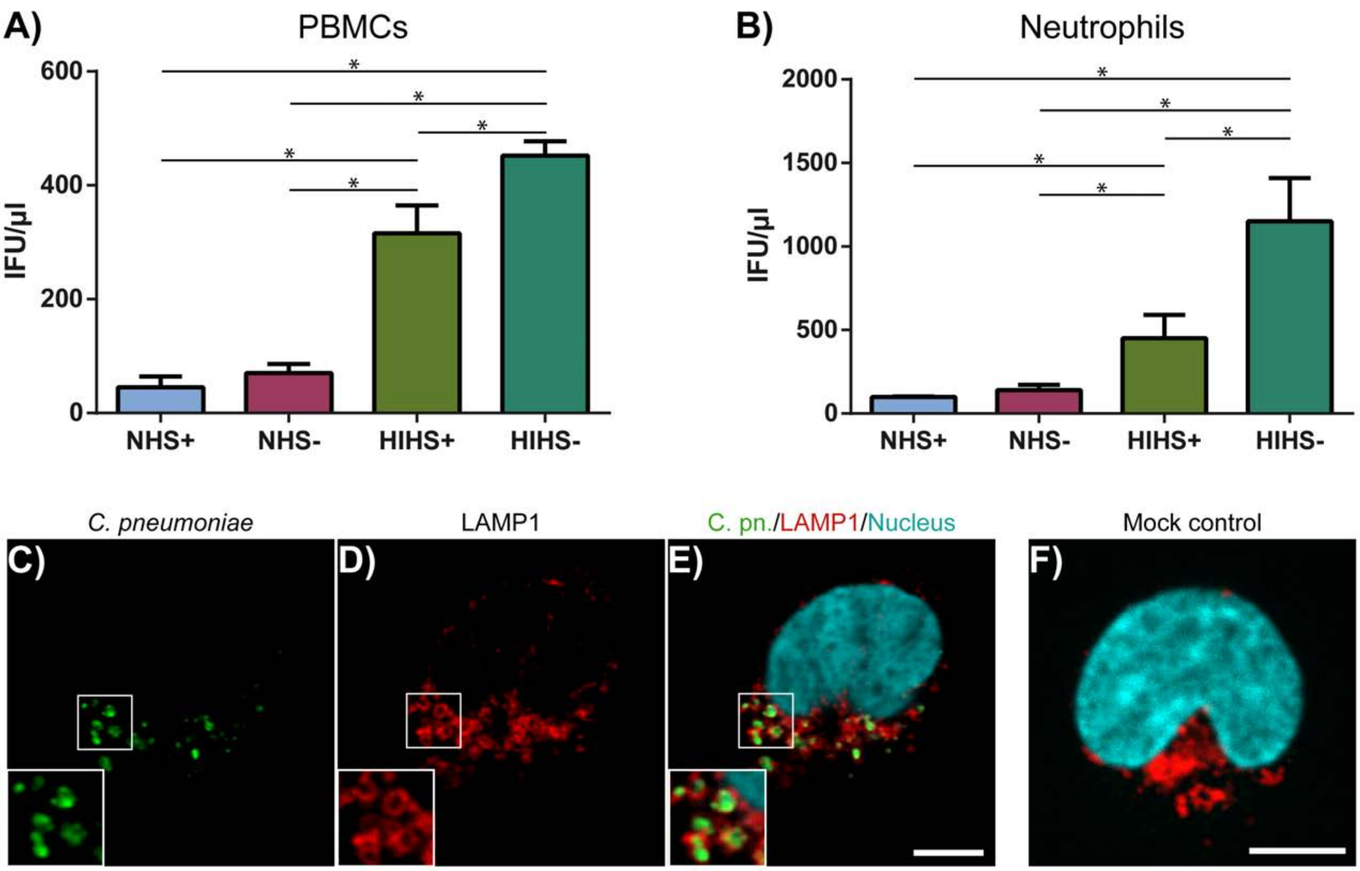
A)
PBMCs
IFU/µl
600
400
200
0
NHS+
NHS-
HIHS+
HIHS-
B)
Neutrophils
IFU/µl
2000
1500
1000
500
0
NHS+
NHS-
HIHS+
HIHS-
C. pneumoniae
LAMP1
C. pn./LAMP1/Nucleus
Mock control
C)
D)
E)
F)